

Efficient second harmonic generation in ZnO nanorod arrays with broadband ultrashort pulses

Susanta Kumar Das,¹ Martin Bock,¹ Christopher O'Neill,¹ Ruediger Grunwald,^{1,a)} Kyung Moon Lee,² Hwang Woon Lee,² Soonil Lee,² and Fabian Rotermund²

¹Max-Born-Institut für Nichtlineare Optik und Kurzzeitspektroskopie, Max-Born-Strasse 2a, D-12489 Berlin, Germany

²Division of Energy Systems Research, Ajou University, Suwon 443-749, Republic of Korea

(Received 18 September 2008; accepted 19 October 2008; published online 6 November 2008)

Broadband frequency-doubling properties of *c*-axis oriented zinc oxide (ZnO) nanorod arrays grown by low-temperature chemical bath method on glass substrate were studied. The maximum effective nonlinearity was found to be about 7.5 times higher than that of a type-I beta-barium borate crystal for a pump intensity of 5.5×10^{10} W/cm². The angular dependence of second harmonic generation (SHG) was determined experimentally. The measured spectral profile of SHG was found to be in good agreement with theoretical simulations. © 2008 American Institute of Physics.

[DOI: 10.1063/1.3021415]

Efficient second harmonic generation (SHG) of broadband femtosecond pulses is important for advanced applications such as pulse characterization, pump/probe spectroscopy, or carrier envelope offset phase measurements. As it was shown in the literature, nanocrystalline zinc oxide (ZnO) films belong to the most promising materials because of specific advantages such as ease and cost-effective manufacturing, less stringent phase-matching requirements,^{1,2} structurally-enhanced frequency conversion by grain boundaries,³ high transmittance in visible-near infrared range, large damage threshold, and chemical stability.⁴ Among the enormous variety of ZnO nanostructures, nanorod geometries enable for generating arrays of well controlled uniformity, shape, and size distribution. Nonlinear optical properties of ZnO nanorods grown by different methods have widely been studied. A considerable enhancement of third-order nonlinearity of ZnO nanorods in comparison to bulk and thin film materials was observed in a previous study.⁵ Several efforts have been made to quantitatively determine the second-order nonlinearity of ZnO nanorod arrays under picosecond excitation.⁶ The microscopic second-order nonlinear coefficient of a single nanorod was measured by near-field scanning optical microscopy.⁷ Our recent results indicate that one can tailor macroscopic second-order nonlinearity by controlling length, diameter, and ordering degree of the nanorods.⁸ Values much higher than for bulk ZnO have been demonstrated with nanorods grown by thermal decomposition.⁹ Due to their higher nonlinearity, ZnO nanorods are more suitable for frequency doubling. Nonlinear excitation of ZnO nanorods at pulse durations in 150 fs range was investigated with particular emphasis on multiphoton absorption channels.¹⁰ However, no systematic and angular resolved investigations of SHG at broadband pulse excitation were reported up to now. In this letter we report on the second-order nonlinear properties of ZnO nanorods induced by exciting with a Ti:sapphire laser oscillator at pulse durations about 13 fs corresponding to spectral full width at half maximum (FWHM) of >100 nm. The effective second-

order nonlinearity (d_{eff}) of ZnO nanorods is estimated. The spectral characteristic of SHG is analyzed both experimentally and theoretically. In our experiments, three different ZnO nanorod arrays were investigated. The nanorods were grown on glass substrates by means of the low-temperature chemical bath method^{11,12} starting from an aqueous solution of zinc nitrate hydrate (ZNH) and hexamethylenetetramine (HMT). A 10 nm thick ZnO layer sputtered onto the glass substrate was used as seed structure. The molar concentrations of ZNH and HMT in distilled water were 30, 60, and 90 mM. In the following we refer to these samples as sample 1, sample 2, and sample 3, respectively. The corresponding average diameters and standard deviations of the nanorods were (56.30 ± 14.55) , (58.77 ± 16.36) , and (95.34 ± 17.24) nm and the average thicknesses were 1300, 870, and 1020 nm. The growth temperature was kept at 95 °C. Scanning electron microscope (SEM) images of the samples are shown in Fig. 1. Hexagonal rods were found to be well aligned in vertical direction (along the *c*-axis). To illuminate the samples, the beam of a Ti:sapphire laser oscillator (Millennia pumped Femtosecure, pulse duration 13 fs,

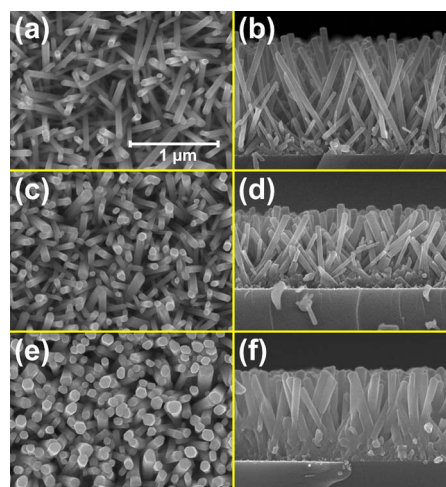


FIG. 1. (Color online) Top- and side-view SEM images of the ZnO nanorod arrays [(a) and (b)]: Sample 1, [(c) and (d)]: Sample 2, [(e) and (f)]: Sample 3, and field of view = $2.53 \times 1.88 \mu\text{m}^2$.

^{a)} Author to whom correspondence should be addressed. Electronic mail: grunwald@mbi-berlin.de.

TABLE I. SHG parameters associated with different samples of ZnO nanorods.

Sample	Thickness (nm)	Diameter of nanorods (nm)	Angle for maximum SHG (deg)	SHG intensity normalized to sample 1	$ d_{\text{eff}} $ (pm/V)
1	1300	(56.30 ± 14.55)	43	1	15
2	870	(58.77 ± 16.36)	29	0.076	2
3	1020	(95.34 ± 17.24)	26	0.21	3.2

linearly polarized, repetition rate 75.3 MHz, pulse energy 2.9 nJ) was focused by an achromatic lens (focal length: 20 mm, thickness: 2 mm, spot diameter: 23 μm) to obtain high efficiencies. The central laser wavelength was 806 nm and the spectral FWHM slightly above 100 nm. The incident peak-on-axis intensity in the focus was 5.5×10^{10} W/cm². In order to find out suitable geometrical conditions for maximum SHG efficiency, the angle of incidence was changed by rotating the sample in two spatial directions. The error resulting from transmission setup and tilting the substrate was regarded to be negligible. The generated SHG signals were analyzed using a spectrometer (HR 2000, Ocean Optics) and an electron multiplying charge coupled device (EMCCD) camera (iXon, Andor Technology). To couple the SHG in the spectrometer fiber (400 μm core diameter), a second imaging lens ($f=5$ cm) was inserted. In case of EMCCD measurement, the SHG was recollimated by a lens of $f=3$ cm. In Table I, the angles of incidence for maximum SHG, spectrally integrated SHG signals (normalized to the value from sample 1), and effective nonlinearities d_{eff} are listed for all samples. The values of d_{eff} for *c*-type crystalline structures mainly result from two individual nonzero nonlinear coefficients d_{311} and d_{333} (Ref. 9).

$$d_{\text{eff}} = d_{311}(\sin \theta_{2\omega} \cos^2 \theta_{\omega} + \cos \theta_{2\omega} \sin 2\theta_{\omega}) + d_{333} \sin \theta_{2\omega} \sin^2 \theta_{\omega}. \quad (1)$$

The peak SHG signal from sample 1 was found to be highest. The absolute value of d_{eff} coefficient of this sample was estimated to be 15 pm/V. The modified Maker Fringe equation^{13,14}

$$P_{\text{shg}} = (512\pi^3/A)d_{\text{eff}}^2 t_w'^4 T_{2\omega} P_{\text{fw}}^2 [1/(n_{\omega}^2 - n_{2\omega}^2)^2] \sin^2 \psi \quad (2)$$

was used for the estimation of the nonlinearity from emission data for an area A . Here P_{shg} and P_{fw} represent the power of SHG and fundamental radiation, respectively. The terms t_{ω} , $T_{2\omega}$ describe the Fresnel field transmission factors for fundamental and SHG. The corresponding phase mismatch factors result from the angles of refraction in the ZnO nanorods (θ'_{ω} , $\theta'_{2\omega}$),

$$\sin^2 \psi = \left(\frac{2\pi L}{\lambda} \right) (n_{\omega} \cos \theta'_{\omega} - n_{2\omega} \cos \theta'_{2\omega}). \quad (3)$$

A ZnO single crystal was used as reference material for this study. Refractive indices for 806 and 403 nm were applied according to the data from Gümüs *et al.*¹⁵ Supposing a d_{eff} value for type-I SHG beta-barium borate (BBO) around 2 pm/V (from SNLO software),¹⁶ the d_{eff} values for sample 1 were determined to be 7.5 times higher than that of BBO. By further comparing the SHG efficiency data to those of a 10 μm thick type-I SHG BBO crystal, the theoretical non-

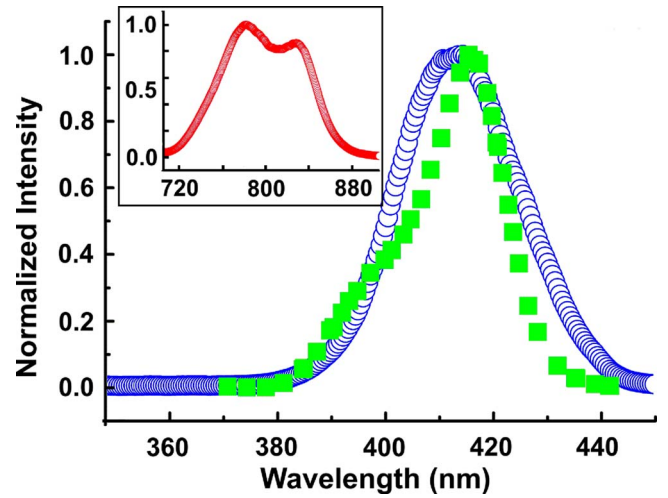


FIG. 2. (Color online) Spectrum of second harmonic radiation (circles: experiment, squares: theory) Inset: spectrum of fundamental radiation corresponding to the pulse duration of about 13 fs.

linear coefficients of ZnO nanorods were also related to experimental values for BBO by empirical calibration factors. The results obtained by this rough estimation confirmed the order of magnitude. The value of d_{eff} for sample 1 is somewhat higher than the reported one for extremely thin ZnO bulk crystal¹⁷ and polycrystalline ZnO thin films.¹⁸ The reported values of d_{eff} exceed five times that of BBO. We assume that the enhancement of the nonlinearity in sample 1 is mainly caused by local field effects similar to the findings for ZnO nanorods at higher aspect ratio (length/diameter).⁹ The SHG spectrum from sample 1 for an incident angle of 43° (corresponding to maximum efficiency in Table I) is shown in Fig. 2. The spectral FWHM of SHG was found to be 27 nm. Although the SHG signal was varying with the angle of incidence (see Fig. 3), its spectral width was found to be nearly constant for all angles. This observation should be explicitly addressed as one of the most interesting results of this study. The comparison of the SHG spectrum to the spectrum of fundamental wave (inset of Fig. 2) enables to evaluate the spectral conversion behavior quantitatively. The bandwidths of both spectra were found to be almost equal (about 0.5×10^{14} Hz). This indicates pulse broadening effects by dispersion and spectral window functions of nonlinear material and/or optical components. It has to be noticed that, although the fundamental spectrum contains two peaks and one valley, only a single peak appears in the SHG spec-

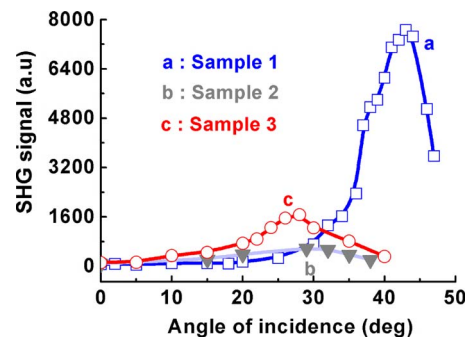


FIG. 3. (Color online) Angular dependence of SHG signal for tilting the plane of the specimen perpendicular to the polarization vector, i.e., p-polarization [(a): Sample 1, (b): Sample 2, and (c): Sample 3].

trum. This discrepancy is not completely understood. Within the large bandwidth of the fundamental, a number of different and contradictory spectrally dependent effects is acting simultaneously (dispersion, Fresnel transmission of the sample, transmission factor of the spectral filter used, etc.) and difficult to separate. The application of aforementioned Marker fringe equation, however, enables to roughly approximate the SHG spectral profile. To estimate the profile function, Eq. (2) was adapted in the form

$$P_{2\omega_i} = (512\pi^3/A)d_{\text{eff}}^2 t_{w_i}^4 T_{2\omega_i}^{\text{BG39}} P_{\omega_i}^2 [1/(n_{\omega_i}^2 - n_{2\omega_i}^2)^2] \sin^2 \psi_i, \quad (4)$$

where P_{ω_i} represents the relative power of the ω_i^{th} frequency component of the fundamental pulse and is defined as

$$P_{\omega_i} = P_{\text{fw}} W(\omega_i), \quad (5)$$

where P_{fw} is the power of fundamental radiation and $W(\omega_i)$ represents a weight factor for the ω_i^{th} component. The term $t_{2\omega_i}^{\text{BG39}}$ stands for the transmission coefficient of a BG39 filter for SHG at the frequency ω_i . The resulting profile was found to be in relatively good agreement with the experimental data as shown in Fig. 2. A detailed analysis of the angular dependence of the SHG signal revealed that the efficiency was not identical for different tilt axes. If the orientation of the axis was parallel to the polarization direction of the fundamental, the efficiency was smaller. The curves in Fig. 3 show the angular dependence for maximum efficiency (tilt axis perpendicular to the polarization vector, i.e., p-p-polarization). Obviously, the angle of maximum SHG depends on structural parameters of the nanorods. In particular, smaller ratios between diameter d of the nanorods and the layer thickness h correspond to larger angles. A similar behavior was reported elsewhere for nanosecond pulse excitation.⁹ A relationship between the ratio d/h and the efficiency can be assumed only for selected samples (e.g., $d/h=0.0433$ and 0.06755 for samples 1 and 2, respectively). For a reliable evidence, however, more and statistically relevant data have to be compared to each other. No multiple photon absorption luminescence^{19,20} was observed in any of the samples for the pump intensity of 5.5×10^{10} W/cm².

To conclude, we studied broadband frequency doubling properties of few cycle Ti:sapphire laser pulses in ZnO nanorods. The maximum effective nonlinearity was found to be about 7.5 times higher than for a type-I SHG BBO crystal. SHG spectrum was analyzed in detail. A dependence on the

tilt axis with respect to the polarization as well as on the geometrical parameters of the nanorods was indicated. Maximum SHG was found for a tilt perpendicularly to the polarization direction of the fundamental. Experiments to improve the accuracy by narrowing the angular spectrum of the focused beam are in progress.

The authors thank T. Elsaesser, W. Seeber, U. Neumann, E. McGlynn, J.-P. Mosnier, I. Kityk, M. Grundmann, and F. Henneberger for useful discussions, M. Tischer and Ch. Poppe for technical assistance, and acknowledge support by DFG (Grant Nos. 1782/2-1 and 1782/7-1) and by KOSEF Grants (Grant Nos. R0A-2007-000-20113-0 and R11-2008-095-01000-0) funded by Korean Government and through the Nanoscopia Center of Excellence at Ajou University.

¹U. Neumann, R. Grunwald, U. Griebner, G. Steinmeyer, and W. Seeber, *Appl. Phys. Lett.* **84**, 170 (2004).

²U. Neumann, R. Grunwald, U. Griebner, G. Steinmeyer, M. Schmidbauer, and W. Seeber, *Appl. Phys. Lett.* **87**, 171108 (2005).

³J. Ebothe, R. Miedzinski, V. Kapustianyk, B. Turko, B. Kulyk, W. Gruhn, and I. V. Kityk, *J. Phys.: Conf. Ser.* **79**, 012001 (2007).

⁴A. B. Djuricic and Y. H. Leung, *Small* **2**, 944 (2006).

⁵H. W. Lee, K. M. Lee, S. Lee, K. H. Koh, J.-Y. Park, K. Kim, and F. Rotermund, *Chem. Phys. Lett.* **447**, 86 (2007).

⁶X. Si, S. Xiong-Rui, L. Chun, H. Yi-Bo, F. Guo-Jia, and W. Qu-Quan, *Chin. Phys. B* **17**, 1291 (2008).

⁷J. C. Johnson, H. Yan, R. D. Schaller, P. B. Peterson, P. Yang, and R. J. Saykally, *Nano Lett.* **2**, 279 (2002).

⁸H. W. Lee, J. T. Kim, K. M. Lee, K. H. Koh, S. Lee, and F. Rotermund, CLEO 2007, paper CThGG4.

⁹S. W. Chan, R. Barille, J. M. Nunzi, K. H. Tam, Y. H. Leung, W. K. Chan, and A. B. Djuricic, *Appl. Phys. B: Lasers Opt.* **84**, 351 (2006).

¹⁰P. Xu, X. Wen, Z. Zheng, G. Coxa, and H. Zhu, *J. Lumin.* **126**, 641 (2007).

¹¹T. Mahalingam, K. M. Lee, K. H. Park, S. Lee, Y. Ahn, J.-Y. Park, and K. H. Koh, *Nanotechnology* **18**, 035606 (2007).

¹²X. Wang, J. Song, and Z. L. Wang, *J. Mater. Chem.* **17**, 711 (2007).

¹³J. Jerphagnon and S. K. Kurtz, *J. Appl. Phys.* **41**, 1667 (1970).

¹⁴M. C. Larciprete, D. Haertle, A. Belardini, M. Bertolotti, F. Sarto, and P. Gunter, *Appl. Phys. B: Lasers Opt.* **82**, 431 (2006).

¹⁵C. Gümüs, O. M. Ozkendir, H. Kavak, and Y. Ufuktepe, *J. Optoelectron. Adv. Mater.* **8**, 299 (2006).

¹⁶SNLO is a public domain software available at AS-Photonics, see <http://www.as-photonics.com/SNLO/>.

¹⁷Y. Kobayashi, D. Yoshitomi, K. Iwata, H. Takada, and K. Torizuka, *Opt. Express* **15**, 9748 (2007).

¹⁸U. Griebner, R. A. Kaindl, T. Elsaesser, and W. Seeber, *Appl. Phys. B: Lasers Opt.* **67**, 757 (1998).

¹⁹C. F. Zhang, Z. W. Dong, G. J. You, R. Y. Zhu, S. X. Qian, H. Deng, H. Cheng, and J. C. Wang, *Appl. Phys. Lett.* **89**, 042117 (2006).

²⁰D. C. Dai, S. J. Xu, S. L. Shi, and M. H. Xie, *Opt. Lett.* **30**, 3377 (2005).